

# Mechanistic and thermodynamic interpretations of zinc sorption onto ferrihydrite

Paras Trivedi,<sup>a,\*</sup> James A. Dyer,<sup>b,c</sup> Donald L. Sparks,<sup>b</sup> and Kaumudi Pandya<sup>d</sup>

<sup>a</sup> Department of Civil and Environmental Engineering, University of Alaska Fairbanks, Fairbanks, AK 99775, USA

<sup>b</sup> Department of Plant and Soil Sciences, University of Delaware, Newark, DE 19717, USA

<sup>c</sup> DuPont Engineering Technology, Brandywine Building, Wilmington, DE 19898, USA

<sup>d</sup> NRL-SRC, National Synchrotron Light Source, Brookhaven National Laboratory, Upton, NY 11026, USA

Received 17 March 2003; accepted 27 May 2003

## Abstract

Elucidating the reaction mechanisms and estimating the associated transport and thermodynamic parameters are important for an accurate description of the fate of toxic metal pollutants, such as Zn(II), in soils and aquatic ecosystems rich in iron oxides. Consequently, sorption of Zn(II) ions onto ferrihydrite was investigated with macroscopic and spectroscopic studies as a function of pH (4.0–8.0), ionic strength ( $10^{-3}$ – $10^{-1}$  M NaNO<sub>3</sub>), aqueous Zn(II) concentration ( $10^{-8}$ – $10^{-2}$  M), and temperature (4–25 °C). Present findings suggest that, for a given set of pH and temperature conditions, Zn sorption onto ferrihydrite can best be described by one average reaction mechanism below the saturation limits. Thermodynamic analyses reveal that the Zn(II) ions sorb onto the ferrihydrite surfaces via strong endothermic chemical reactions. Consistently, X-ray absorption spectroscopic (XAS) analyses confirm that, at pH < 6.5, for all Zn loadings, Zn(II) ions form corner-sharing, mononuclear, bidentate inner-sphere complexes with ferrihydrite, where  $R_{\text{Zn-O}} \approx 1.97$  Å and  $R_{\text{Zn-Fe}} \approx 3.48$  Å. For pH ≥ 6.5, similar sorption complexes were observed at lower sorption densities. Then again, for pH ≥ 6.5 and at higher sorption densities, Zn(II) ions may begin to form zinc-hydroxide-like polynuclear sorption complexes on the surfaces of the ferrihydrite, where  $R_{\text{Zn-Zn}} \approx 3.53$  Å. Surprisingly, small changes in temperature had a significant impact on the affinity of zinc for the ferrihydrite surface; equilibrium sorption capacity decreased by 3–4 orders of magnitude as temperature fell from 25 to 4 °C for all pH. Zinc sorption onto ferrihydrite, therefore, is governed by pH as well as by temperature and sorbate/sorbent ratio.

© 2003 Elsevier Inc. All rights reserved.

**Keywords:** Zn(II); Ferrihydrite; Sorption; Thermodynamics; XAS

## 1. Introduction

The mobility and bioavailability of anthropogenically released trace metal contaminants, such as Zn(II), in aquatic and soil ecosystems are of great ecological concern. In these ecosystems, interactions of metal contaminants with ubiquitously existing hydrous oxides of Fe, Al, and Mn as well as with clays and clay minerals are important, because they directly control contaminant distribution and transport. In most natural systems, Zn(II) ions can successfully form complexes with clay minerals [1,2]; aluminum hydr(oxides) [3–6]; manganese oxides [6,7]; and iron oxides [4–6,8–11]. Direct synchrotron-based investiga-

tions have supported the conclusions of traditional chemical analyses that iron oxides and oxyhydroxides in these ecosystems serve as major sinks for zinc [12–17].

The nature of the sorption complexes is largely dependent on the nature of the sorbent and on the zinc species present in these systems. Crystalline oxides, such as goethite, exhibit higher adsorption energies than amorphous hydrous Fe oxides [11,18,19]. Consistently, Zn(II) ions retain their primary hydration shell when sorbed onto amorphous hydrous oxides of iron [20] and manganese [21], and thus they form outer-sphere complexes. On the other hand, inorganic Zn(II) forms inner-sphere complexes with other sorbents, such as crystalline aluminum [22] and iron oxides (goethite) [20,23]; metastable iron oxides such as ferrihydrite [24]; and other crystalline minerals, such as calcite [25]. In contrast, Schlegel et al. [23] observed that zinc

\* Corresponding author.

E-mail address: [paras.trivedi@uaf.edu](mailto:paras.trivedi@uaf.edu) (P. Trivedi).

ions complexed with EDTA retained their octahedral hydration shells upon sorption onto goethite. Then again, at high loadings, with Al-bearing minerals, such as pyrophyllite [2] and alumina [22], Zn(II) binds chemically to form hydrotalcite-like complexes, whose crystalline stability increases with reaction time. Overall, these studies demonstrate that the nature of zinc sorption complexes depends on the physical and chemical properties of sorbents as well as on the concentrations and the forms of Zn(II) species. Interestingly, on a long-term basis, Zn(II) ions continue to migrate into the micropores of the sorbent oxides via intraparticle diffusion, where the sorption mechanism has been found not to change from the one observed on the external surface [6,9,21].

Recently, Waychunas et al. [24] provided significant insight into the mechanisms controlling the sorption of Zn(II) ions onto 2-line ferrihydrite in the neutral pH range under multiple reaction conditions. They found that Zn(II) ions form inner-sphere bidentate complexes with ferrihydrite at lower sorption densities, while they form surface precipitates of zinc-hydroxide-like polymers at higher sorbate loadings [24]. Although the second shell surrounding the tetrahedrally coordinated sorbed Zn(II) ion is surrounded by as many as four Fe neighbors in the coprecipitates versus two Fe neighbors in the sorption complexes, the average Zn–Fe bond distance was approximately 3.44 Å in all systems. Given the complex chemistry of aqueous Zn(II) species [24], the interactions between Zn(II) and ferrihydrite in aquatic ecosystems can be highly sensitive to changes in pH, ionic strength, sorbate/sorbent ratio, and changes in temperature. In order to identify the mechanisms that significantly control the Zn(II)-ferrihydrite interactions, there is a strong need to investigate these reactions over a wide pH range (4.0–8.0) as a function of varying zinc loadings ( $10^{-8}$ – $10^{-4}$  M  $\text{Zn}(\text{NO}_3)_2$ ) and varying ionic strengths ( $10^{-3}$ – $10^{-1}$  M  $\text{NaNO}_3$ ). Additionally, changes in temperature can significantly alter the nature of these sorption reactions [6,10,26]. Thermodynamic parameters, such as adsorption enthalpy and entropy, can provide a much clearer picture of the driving forces involved in the sorption reactions, and they can serve as important tools for developing accurate predictive models.

The primary objective of this research paper, therefore, is to elucidate these mechanisms by conducting a systematic set of macroscopic studies complemented with X-ray absorption spectroscopic analyses over a wide range of pH, Zn(II) concentrations, ionic strength, and temperature. Macroscopic studies will be employed to assess the effect of different factors controlling the sorption of Zn(II) ions onto ferrihydrite as well as to estimate important transport and thermodynamic parameters that can be used for predicting the fate of Zn(II) ions in aquatic ecosystems. The results from X-ray absorption spectroscopy (XAS) studies will assist in revealing the mechanisms responsible for the sorption reactions. In addition, these mecha-

nisms will be used to support surface complexation modeling of the macroscopic data in the companion paper [27], the results of which will be used in another companion paper to simulate and validate Zn(II) removal in multi-stage aqueous waste treatment systems [28]. Combining molecular-scale research with macroscopic and thermodynamic modeling over a wide range of reaction conditions is significant, because it provides a systematic and thorough approach to understanding the speciation and fate of aqueous Zn(II) in the presence of hydrated iron oxides.

## 2. Materials and methods

### 2.1. Macroscopic studies

All the experimental procedures are conducted under closed system conditions (in the  $\text{N}_2$  glovebox) and turbulent hydraulic conditions ( $Re \geq 2.9 \times 10^5$  with respect to reactor diameter). All the experiments used ACS reagent-grade chemicals, double-deionized water, and acid-washed polypropylene reactors. Ferrihydrite was prepared per the procedure detailed by Trivedi et al. [29]. The adsorbent's physical and chemical characteristics have been described previously [29,30]. Traditional sorption edge and isotherm studies were conducted in 250-ml high-density polyethylene (Nalgene) containers with  $1 \text{ g l}^{-1}$  oxide to assess the amount of contaminant sorbed to the iron oxide as a function of pH (4.0–8.0), ionic strength ( $10^{-3}$ – $10^{-1}$  M  $\text{NaNO}_3$ ), solution concentration ( $10^{-8}$ – $10^{-2}$  M  $\text{Zn}(\text{NO}_3)_2$ ), and temperature (4–25 °C). The solution concentrations of Zn(II) were maintained below the solubility limits [31] for  $\text{Zn}(\text{OH})_2$  and ZnO. To evaluate maximum sorption capacities, additional isotherm studies were conducted with a  $0.1 \text{ g l}^{-1}$  oxide suspension. Preliminary batch studies were conducted to assess the kinetics of Zn sorption onto the external surfaces of the ferrihydrite particles under different pH conditions and under the boundary conditions similar to the ones employed in traditional isotherm studies. Under these boundary conditions, a contact time of 4 h is sufficient for equilibration of Zn sorption onto the external surface as well as onto the macropore walls of the ferrihydrite particles. Furthermore, contributions from intraparticle diffusion of Zn(II) ions along the micropore walls of ferrihydrite will be insignificant under these boundary conditions [6,29]. Samples were collected and filtered using 0.2- $\mu\text{m}$  Gelman Supor-200 filters. The filtrate was acidified and analyzed with graphite-furnace atomic absorption spectroscopy (Perkin–Elmer Analyst 800) to determine the bulk aqueous Zn(II) concentrations. For XAS analyses, suspensions from 25 °C studies were centrifuged at 12,000 g for 20 min to ensure maximum solid–liquid separation. Resultant wet pastes were immediately loaded into acrylic sample holders, which were sealed with Mylar windows to prevent the loss of moisture.

## 2.2. XAS data collection

XAS data were acquired on beamline X-11A at the National Synchrotron Light Source (NSLS), Brookhaven National Laboratory where the electron beam energy was 2.528–2.8 GeV with a maximum beam current of 280 mA. Prior to data collection, the beam energy was calibrated to the first inflection point of the Zn metal foil ( $E_0 = 9.659$  keV). The XAS data for the Zn–ferrihydrite sorption samples were collected at the ZnK-edge over the energy range of 9.459–13.915 keV in fluorescence mode using a Lytle detector. The samples were placed  $45^\circ$  to the incident beam. Harmonic rejection was achieved by detuning the monochromator at least 30% of  $I_0$ . For each sample, multiple scans were collected to improve the signal-to-noise ratio. The XAS data for the reference compounds including 1.0 mM aqueous solution of  $\text{Zn}(\text{NO}_3)_2$  at pH 2.0 and ZnO were collected over the ZnK-edge in transmission mode.

The XAS spectra were analyzed using WinXAS (Version 2.1). For each scan, the background X-ray absorbance was subtracted by fitting a linear polynomial through the pre-edge region. The edge jump of a background corrected spectrum was normalized with a linear polynomial over 9.759–9.959 keV. The threshold energy ( $E_0$ ) was determined from the first inflection point in the edge region and was used to convert the spectra from energy to  $k$ -space. A cubic spline function was employed to account for the atomic absorption in the absence of backscattering contributions over the range 2.0–10.0  $\text{\AA}^{-1}$ . This isolated function produced the XAFS function ( $\chi(k)$ ), which was then weighted by  $k^3$  to enhance the higher  $k$ -space data. The Bessel window function was used in Fourier transforms to produce the radial structural function (RSF) over 2.4–9.2  $\text{\AA}^{-1}$  for all sorption samples. These RSFs are uncorrected for phase shifts.

To obtain the structural information, the Fourier transforms were fit with a Fe-substituted chalcophanite ( $\text{ZnMn}_3\text{O}_7 \cdot 3\text{H}_2\text{O}$ ) model generated using FEFF7 [32], where all the parameters, except the amplitude reduction factor ( $S_0^2$ ), were allowed to float. A comparison of the  $\text{Zn}(\text{NO}_3)_2$  solution spectra collected in transmission mode with that of the fluorescence mode revealed an average amplitude reduction factor ( $S_0^2$ ) of 0.70, which was used in fitting. In each sample, the  $E_0$  shift was constrained to be equivalent for all shells. The number of parameters varied during the fitting was always less than the maximum allowed based on  $N_{\text{free}} = (2 \times \Delta k \times \Delta R) / \pi$ , where  $N_{\text{free}}$  is the number of degrees of freedom,  $\Delta k$  is the range of  $k$ -space being fit, and  $\Delta R$  is the range of the  $R$ -space. For any given shell, a good fit was established by minimizing the residual error. Additionally for each sample, the fitting routine was carried out on their individual scans as well as their averaged scan to account for the analytical errors. For all samples, the errors associated with the structural parameters did not exceed  $\pm 20\%$ .

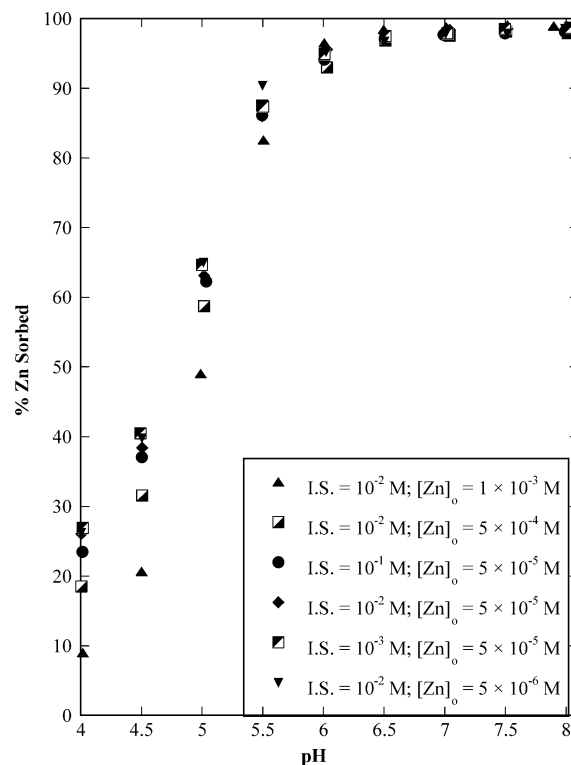


Fig. 1. pH edges of Zn(II) sorption onto ferrihydrite ( $1 \text{ g l}^{-1}$ ) at  $25^\circ \text{C}$  and under closed system conditions: effect of ionic strength and initial Zn(II) concentrations.

## 3. Results and discussion

### 3.1. Macroscopic analyses

The sorption edges of Zn(II) sorbed onto ferrihydrite, as seen in Fig. 1, follow a sigmoid profile. This profile is a characteristic of Zn(II) and is consistent with the ones observed by others [4,6,11,18,19,33–36]. At all  $\text{pH} > 4.5$ , the percent of Zn(II) sorbed onto ferrihydrite is independent of the ionic strength, which suggests chemisorption as the dominant mechanism. Zn sorption onto goethite is also found to be independent of ionic strength as well as of sorbate/sorbent ratios employed in the adsorption edge studies [4,11].

To assess the effect of adsorbate concentrations on Zn(II) sorption to ferrihydrite, traditional isotherm studies were conducted at pH 4.5, 5.5, 6.5, and 7.5 under closed system conditions at multiple temperatures (Fig. 2). In all isotherms, as the sorbate/sorbent ratio increases, the isotherm begins to plateau, indicating the onset of maximum possible coverage of the sorption sites available on the surface of ferrihydrite. Below this level of site saturation, the amount of Zn(II) sorbed is linearly proportional to the corresponding aqueous bulk concentration. Therefore, Zn(II) sorption onto ferrihydrite can be modeled with one average type of site. Recently, Criscenti and Sverjensky [37] demonstrated that sorption of cations, such as Cd(II) and Zn(II), onto hydrous ferric oxide can be accounted for with the help of a single-site triple-layer model. Surface complexation modeling of

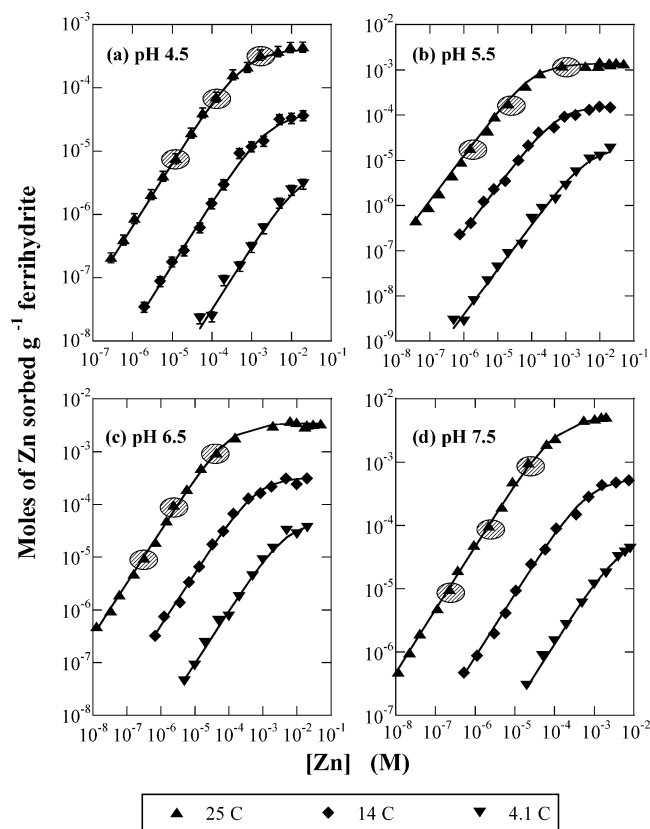


Fig. 2. Isotherms of Zn(II) sorption onto ferrihydrite ( $1 \text{ g l}^{-1}$ ) under closed system conditions at  $25^\circ\text{C}$  and I.S.  $10^{-2} \text{ M}$  of  $\text{NaNO}_3$ ; effect of pH and temperature. Solid points represent experimental data and the lines represent single-site Langmuir fits employed to evaluate the adsorption enthalpies in Fig. 3. Langmuir model parameters presented in Table 1. XAS studies were conducted on data points marked with ovals.

the macroscopic sorption data from the present studies is discussed in detail in a companion paper [27].

Temperature fluctuations of  $20^\circ\text{C}$  or more (as a result of seasonal variations) are not uncommon in natural systems. These changes in temperature can significantly alter the sorption properties of the sorbent as well as the chemistry of the adsorbates, and hence they will affect the sorption of the metal contaminants in the natural environment. For example, as shown in Fig. 2, the capacity of ferrihydrite for zinc at a fixed equilibrium aqueous Zn(II) concentration decreases by 3–4 orders of magnitude as the temperature falls from  $25$  to  $4^\circ\text{C}$  for all pH. These results suggest that even small changes in temperature can significantly alter the distribution and mobility of metal ions in soils and aquatic sediments that contain significant fractions of iron oxides. Furthermore, these temperature variations will significantly impact the performance of wastewater treatment systems that employ iron oxides, such as ferrihydrite, as metal scavengers. Thus, there is a need for thermodynamic analysis of a sorption system, as it provides a clearer picture of the driving forces involved and also serves as a useful tool for predicting the fate of metal contaminants in natural environments.

Even though the single-site Langmuir model is limited, in the sense that it does not explicitly account for the electrostatic charges on the mineral surfaces, it is employed here to fit the isotherm data strictly for estimating the thermodynamic parameters. The resulting Langmuir isotherm equilibrium constants ( $K$ ) are employed in the van't Hoff model to estimate the adsorption enthalpies of Zn sorption onto ferrihydrite as a function of pH [38]. Because Zn(II) sorption onto ferrihydrite increases with increasing temperature, the sorption is endothermic. The adsorption enthalpies (Table 1 and Fig. 3), suggest that Zn(II) ions may chemisorb to ferrihydrite [38], where the sorption reaction is provoked by the bond formation. The adsorption enthalpies in Fig. 3 are slightly smaller than the ones observed for goethite, which were found to be about  $33 \text{ kcal mol}^{-1}$  [6], but much greater than the ones observed for surfactant-modified montmorillonite [39] and amorphous hydrous oxides of Al, Fe, and Mn, where the adsorption enthalpies were less than  $25 \text{ kcal mol}^{-1}$  [6]. These results corroborate the hypothesis that the relative binding strength of crystalline oxides, such as goethite, for metals is much greater than that of nanocrystalline materials, such as ferrihydrite and highly amorphous hydrous ferric oxide gels [11,18,19]. Rodda et al. [10] noted that the increase in Zn(II) sorption onto goethite with increasing temperature is also a function of pH. Bayat [40] investigated Cd(II) and Zn(II) sorption onto fly ash, which contained 3.30 wt% of iron oxide and estimated adsorption enthalpies to be  $40.2 \text{ kcal mol}^{-1}$  for Zn(II) and  $10.44 \text{ kcal mol}^{-1}$  for Cd(II). Likewise, the adsorption enthalpies for Cd(II) sorption onto goethite [41] and onto kaolinite [42] were significantly altered with changes in pH.

Furthermore, based on the equilibrium constants presented in Table 1, the standard state Gibbs free energies ( $\Delta G^0$ ) for the sorption reactions were estimated. These energies, ranging from  $-2.22$  to  $-5.40 \text{ kcal mol}^{-1}$ , are much smaller in magnitude than the one estimated by Zhu [43] for the surface precipitation of Zn(II) onto hydrous ferric oxide (HFO), which is approximately  $-13.916 \text{ kcal mol}^{-1}$ . These results suggest that surface precipitation may not be a significant contributor in the present systems. The positive values of entropies ( $\Delta S^0$ ) (Table 1) show the increased randomness at the solid/solution interface during adsorption. Given the errors, the entropies (Table 1) did not vary significantly with pH and temperature, suggesting that the net sorption mechanism may be independent of these parameters [10]. Furthermore, the small entropies indicate that the ferrihydrite structure did not change significantly as a result of adsorption.

The estimated maximum sorption capacities of ferrihydrite (Table 1) range from  $10^{-4}$  to  $10^{-3}$  moles of Zn  $\text{g}^{-1}$  of ferrihydrite. These sorption capacities are smaller than those observed for amorphous ferric oxide gels [19,20], but they are one order of magnitude greater than those reported for goethite [4,10,11]. These differences in the sorption capacity can be attributed to two critical factors that define the nature

Table 1  
Thermodynamic parameters of zinc sorption onto ferrihydrite based on the single-site Langmuir model

$T$ ( $^{\circ}\text{C}$ )	$K^{\text{a,b}}$ ( $\text{l mol}^{-1}$ )	$\Gamma_{\text{max}}^{\text{a,b}}$ ( $\text{mol g}^{-1}$ )	$\Delta G^{0\text{b,c}}$ ( $\text{kcal mol}^{-1}$ )	$\Delta H^{0\text{b,d}}$ ( $\text{kcal mol}^{-1}$ )	$\Delta S^{0\text{b,e}}$ ( $\text{kcal mol}^{-1} \text{K}^{-1}$ )
pH 4.5					
24.6	1571	$4.08 \times 10^{-4}$	-4.36		0.105
14.0	388.6	$4.06 \times 10^{-5}$	-3.40	26.91	0.106
4.1	56.67	$5.60 \times 10^{-6}$	-2.22		0.105
pH 5.5					
24.7	9091	$1.39 \times 10^{-3}$	-5.39		0.120
14	1707	$9.62 \times 10^{-5}$	-4.24	30.42	0.121
4.1	201.6	$1.92 \times 10^{-5}$	-2.92		0.120
pH 6.5					
24.4	9206	$3.45 \times 10^{-3}$	-5.40		0.121
14.1	1550	$3.23 \times 10^{-4}$	-4.20	30.73	0.122
4.1	203.9	$4.72 \times 10^{-5}$	-2.93		0.121
pH 7.5					
24.9	9015	$5.21 \times 10^{-3}$	-5.39		0.122
14	1483	$5.62 \times 10^{-4}$	-4.17	31.00	0.122
4.1	194.5	$7.05 \times 10^{-5}$	-2.91		0.122

<sup>a</sup> Based on the single-site Langmuir isotherm,  $1/C = 1/(K \times \Gamma_{\text{max}} \times S) + 1/\Gamma_{\text{max}}$ , where  $C$  = moles Zn sorbed  $\text{g}^{-1}$  ferrihydrite,  $S$  = M Zn in bulk aqueous phase at equilibrium,  $K$  = equilibrium constant, and  $\Gamma_{\text{max}}$  = maximum sorption capacity.

<sup>b</sup> An error of  $\pm 11\%$  is associated with the parameter.

<sup>c</sup>  $\Delta G^0$  represents the Gibbs free energy.

<sup>d</sup>  $\Delta H^0$  represents adsorption enthalpy.

<sup>e</sup>  $\Delta S^0$  represents change in adsorption entropy.

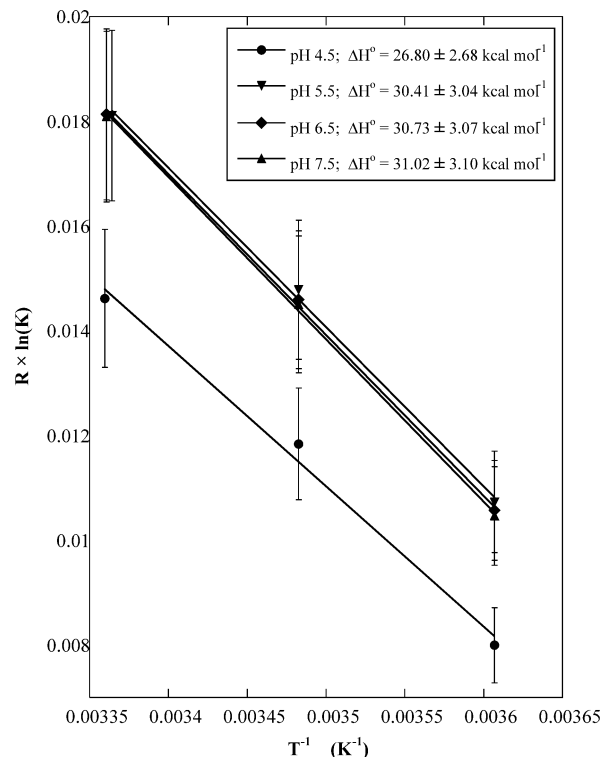


Fig. 3. Estimation of enthalpies associated with Zn(II) sorption onto ferrihydrite as a function of pH. The values of the adsorption equilibrium constants ( $K$ ) were obtained by fitting the isotherm data with a single-site Langmuir model (Fig. 2). Solid lines represent the van't Hoff model and the slopes of these lines provide the adsorption enthalpies.

of iron oxides/oxyhydroxides—the method of preparation and the aging period. Interestingly, even the maximum sorption capacities determined from the single-site Langmuir model (Table 1) are increasing with temperature, indicating an increase in the active sorption sites with temperature. Consistently, Rodda et al. [10] found that the sorption capacities for Zn(II) on goethite increased with pH as well as with temperature. These results suggest that even small changes in the system temperature will significantly impact the sorbent loadings required by wastewater treatment systems that employ ferrihydrite for the removal of aqueous metal contaminants.

### 3.2. XAS analyses

The peaks in XAS spectra of Zn–ferrihydrite sorption complexes studied at pH 4.5 (Fig. 4a), 5.5 (Fig. 4b), 6.5 (Fig. 4c), and 7.5 (Fig. 4d) and under varying adsorbate concentrations are much broader than that of  $\text{Zn}^{2+}$  in aqueous solution suggesting sorbed Zn(II) ions may not retain their primary hydration shell. These spectra have a noisy and have a beat pattern indicative of at least two different neighbors surrounding the sorbed Zn(II) ion. Based on XANES analyses, Waychunas et al. [44] found that octahedrally coordinated aqueous Zn(II) species sorb as tetrahedral complexes onto ferrihydrite. The highly disordered ferrihydrite in the background causes these sorption spectra (Fig. 4) to be noisier in the higher  $k$  region. Although the  $\chi$  spectra of Zn–ferrihydrite sorption complexes are similar under all reaction conditions, they are less noisy at higher pH values

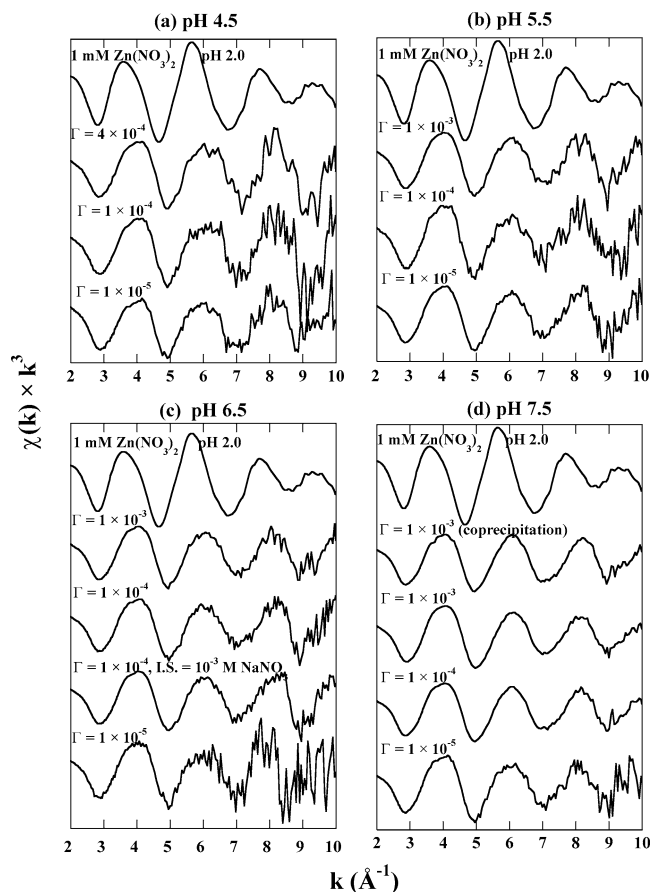


Fig. 4. Background subtracted, normalized, averaged ZnK-edge XAS spectra of Zn-ferrihydrate complexes at 25 °C, and I.S.  $10^{-2}$  M  $\text{NaNO}_3$  under closed system conditions: effect of Zn sorption density ( $\Gamma$  mol of Zn sorbed  $\text{g}^{-1}$  ferrihydrate) and mode of reaction at pH (a) 4.5, (b) 5.5, (c) 6.5, and (d) 7.5. The spectra for the sorption samples are compared with the averaged ZnK-edge XAS spectrum of 1 mM aqueous  $\text{Zn}(\text{NO}_3)_2$  solution at pH 2.

and their signal-to-noise ratios improved with the sorbate concentrations. Furthermore, these sorption spectra do not resemble those of  $\text{ZnO}$  or  $\text{ZnCO}_3$  [16,20], thus ruling out the possibility of the formation of these precipitates.

The Fourier transforms of the sorption samples (Figs. 5a–5d), which are uncorrected for the phase shift, show two distinct shells surrounding the sorbed Zn(II) ion. Results of the fitting analyses (Table 2) obtained as a result of considering only single scattering from the first and second shell contributions show that the first shell surrounding the sorbed Zn(II) ion is composed of approximately four oxygens with an average Zn–O bond distance of 1.97 Å. This first shell coordination is consistent with the ones observed for Zn sorption complexes with goethite [20], ferrihydrate [24], and alumina powders [22], and it suggests that Zn(II) ions lose their octahedral primary hydration shell to sorb onto ferrihydrate surfaces as tetrahedral units. Previous extensive compilations of the local structures of Zn reference compounds show that aqueous Zn(II) ions have octahedral first shell coordinations with Zn–O distances ranging

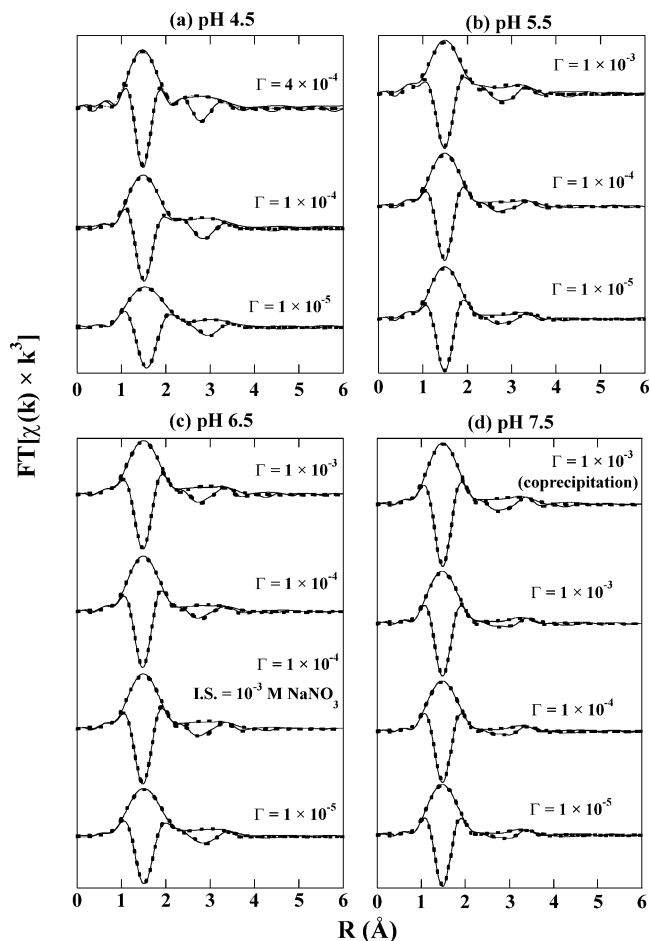


Fig. 5. Fourier transforms (magnitude + real part) of ZnK-edge XAS spectra (solid lines) of Zn-ferrihydrate sorption complexes presented as a function of Zn sorption density ( $\Gamma$  mol of Zn sorbed  $\text{g}^{-1}$  ferrihydrate) at pH (a) 4.5, (b) 5.5, (c) 6.5, and (d) 7.5. All spectra are filtered over  $k$ -range 2.1–9.2  $\text{\AA}^{-1}$  and fitted with a theoretical model of Fe-substituted chalcanthite (dashed lines) from 0.7 to 3.9 Å. Fitting results shown in Table 2.

from 2.10–2.18 Å, whereas most zinc oxides and hydroxides have a tetrahedral unit with an average Zn–O distance ranging from 1.96–1.99 Å [20,24]. Accordingly, the Zn(II) ions sorbed onto ferrihydrate do not appear to retain their primary hydration shell, suggesting that electrostatic forces may not drive these sorption reactions. Trainor et al. [22] observed that at low sorption densities ( $<1.1 \mu\text{mol m}^{-2}$ )  $\text{Zn}^{2+}$  sorbs to alumina as a mononuclear inner-sphere complex with tetragonal first shell coordination and an average Zn–O distance of 1.96 Å. They [22] also observed two additional oxygen atoms in the first shell at the higher sorption densities; however, they argue that given the short Zn–O distances (2.01–2.04 Å) in the first shell, these additional oxygens may be from the alumina surface resulting in distorted octahedra. In contrast, Zn sorbed to pyrophyllite [2], amorphous HFO [20], goethite [23], and HMO [21] appeared to retain its octahedral oxygen coordination. In iron oxides, the reactivity of Zn(II) is dependent not only on the degree of disorder of the sorbents but the method of preparation and the aging of the oxides. For example, aqueous Zn(II) ions

were found to be physically sorbed onto a highly disordered freshly precipitated HFO gel [20]. In contrast, Zn(II) ions lose their waters of hydration when sorbed onto two-line ferrihydrite aged for 24 h [24], a two-line ferrihydrite aged for 48 h (present study), and highly crystalline goethite [20]. Likewise, the differences in the local structures of Zn(II) sorbed onto goethite as observed by Schlegel et al. [23] and by Trivedi et al. [20] can arise from the degree of oxide crystallinity. Because the Zn–O distances in zinc carbonates are also consistent with octahedral coordination [20, 24], they are much larger than ones observed in the present Zn–ferrihydrite sorption complexes. Hence, the possibility of the formation of zinc-carbonate-like surface precipitates can be excluded from the present systems.

In the sorption complexes studied at pH 4.5 and 5.5, the second shell was best fit with approximately two Fe atoms at an average bond distance of  $3.48 \pm 0.01$  Å (Table 2). Inclusion of Zn as second-shell neighbors, with or without Fe atoms, did not provide any stable fits, which is indicative of insignificant contributions from multinuclear Zn precipitates. Given the uncertainty of 0.05 Å in the Zn–Fe bond distances, these results are consistent with the ones observed for various Zn–iron oxide systems, where the sorbed Zn(II) ions form corner-sharing bidentate complexes with the octahedral Fe units [20,24]. In contrast, a number of other studies [14,23] reported a much smaller Zn–Fe bond distance of  $3.12 \pm 0.1$  Å. Schlegel et al. [23] attributed these short distances to an edge linkage between the Zn octahedra and the Fe octahedra on the goethite surface. Thus the present analyses insinuate that, at  $\text{pH} \leq 5.5$ , Zn(II) ions predominantly bind via chemical forces with ferrihydrite to form corner-sharing mononuclear bidentate complexes, which confirms chemisorption as suggested from the thermodynamic analyses of the macroscopic studies. Furthermore, at these pH values, the local structure of the sorbed Zn(II) ion is independent of the sorbate/sorbent ratio, which is indicative of one average type of sorption mechanism. This information is very important and will assist in the surface complexation modeling of the isotherm data [27].

At pH 6.5 and 7.5, for the low sorption densities, Zn(II) ions are observed to form sorption complexes (Table 2) similar to the ones observed at lower pH values. Trainor et al. [22] also found Zn(II) forming predominantly mononuclear complexes with alumina at pH 7.0 and 8.0 at lower sorption densities. Interestingly, for the highest Zn loadings at pH 6.5 as well as for most Zn–ferrihydrite sorption complexes studied at pH 7.5, the second shell can be successfully fitted with either Fe atoms alone at an average bond distance of 3.48 Å or with a Zn atom at an average bond distance of 3.53 Å along with the Fe atoms at an average radial distance of 3.47 Å. Based on the X-ray photoelectron spectroscopic (XPS) measurements on dried samples of Zn-hydrous ferric oxide sorption complexes, Harvey and Linton [45] observed a similar change in the speciation from monolayered chemisorbed coverage at  $\text{pH} < 6.5$  to Zn(OH)<sub>2</sub>-like precipitates at higher pH and higher sorption densities. For the

Zn–Fe coprecipitate studied at pH 7.5 (Table 2), the second shell was best fit only when contributions from Zn as well as from Fe were included. No meaningful fits were obtained when Zn was considered as the only second shell neighbor; thus the evidence for the formation of Zn precipitates could not be established. When Fe atoms were considered as sole contributors to the second shell, the local structures of the Zn–ferrihydrite complexes (Table 2) do not appear to vary with pH or the sorbate/sorbent ratio. Manceau et al. [46] aged a Zn–ferrihydrite coprecipitate under alkaline conditions and at 70 °C to form a Zn-substituted goethite. An XAS analysis revealed the second shell to be composed of Fe atoms with Zn–Fe bond distances ranging from 3.0 to 3.48 Å [46]. With alumina, at higher Zn sorption densities, the Zn–Zn contributions increase, while the Zn–Al contributions remain unaltered, suggesting the formation of a hydroxalite-like mixed metal coprecipitate [22].

In the second scenario, where the second shell is fitted with Fe and Zn, the weak Zn–Zn contributions suggest that, with increases in pH and Zn loading, Zn(II) ions may begin to form corner-sharing polynuclear complexes on the surface of ferrihydrite. Furthermore, the Zn–Zn and the Zn–Fe distances are consistent with the ones observed in franklinite as well with those in Zn–ferrihydrite systems studied by Waychunas et al. [24] for similar Zn loadings studied under similar reaction conditions. However, the analyses of the bulk spectra do not provide any evidence for the formation of any well-known Zn precipitates. If there are any precipitates forming, then their contributions to the average local structure are very small. Concurrently, the thermodynamic analyses presented earlier (Table 1) suggested that surface precipitation may not be a significant contributor to the overall uptake of Zn(II) by ferrihydrite. At Zn loadings higher than the ones studied in the present research, Waychunas et al. [24] observed that these polynuclear complexes serve as the precursors for a more stable zinc-hydroxide-like precipitate.

#### 4. Summary

In this research, macroscopic studies are complemented with X-ray absorption spectroscopy to investigate the sorption interactions between inorganic Zn(II) ions and ferrihydrite over a wide range of reaction conditions pertinent to natural aquatic environments. Traditional macroscopic studies suggested that one average sorption mechanism can adequately describe Zn(II) complexation with ferrihydrite. Thermodynamic parameters, derived from single-site Langmuir model, are broadly indicative of endothermic chemical reactions between Zn(II) ions and the sorption sites on the ferrihydrite surfaces. Consistently, X-ray absorption spectroscopic (XAS) analyses confirm that, for  $\text{pH} < 6.5$  and at all Zn loadings, Zn(II) ions form corner-sharing, mononuclear, bidentate inner-sphere complexes with ferrihydrite. At  $\text{pH} \geq 6.5$ , similar sorption complexes were ob-

Table 2  
Structural parameters of Zn(II)–ferrihydrite sorption complexes from XAS analyses

pH	$\Gamma$ (mol g <sup>-1</sup> )	Atom <sub>1</sub>	$N_1^a$	$R_1$ (Å) <sup>b</sup>	$\sigma_1^2$ (Å <sup>2</sup> ) <sup>c</sup>	Atom <sub>2</sub>	$N_2^a$	$R_2$ (Å) <sup>b</sup>	$\sigma_2^2$ (Å <sup>2</sup> ) <sup>c</sup>	$\Delta E^0$ (eV)	% Res.
4.5	$4 \times 10^{-4}$	O	4.80	1.988	0.0047	Fe	1.87	3.495	0.0110	2.11	7.48
4.5	$1 \times 10^{-4}$	O	4.25	1.986	0.0053	Fe	1.90	3.473	0.0117	1.89	6.61
4.5	$1 \times 10^{-5}$	O	4.61	1.986	0.0056	Fe	2.24	3.484	0.0131	2.37	7.44
5.5	$1 \times 10^{-3}$	O	4.07	1.975	0.0047	Fe	2.23	3.471	0.0094	2.56	6.37
5.5	$1 \times 10^{-4}$	O	3.84	1.971	0.0053	Fe	1.99	3.482	0.0110	2.43	3.02
5.5	$1 \times 10^{-5}$	O	4.11	1.977	0.0057	Fe	2.14	3.474	0.0122	1.79	7.28
6.5	$1 \times 10^{-3}$	O	4.07	1.965	0.0048	Fe	2.27	3.481	0.0124	2.29	6.89
						Fe <sup>f</sup>	1.75	3.474	0.0110	3.25	8.31
						Zn <sup>f</sup>	0.17	3.527	0.0110		
6.5	$1 \times 10^{-4}$	O	3.89	1.971	0.0051	Fe	2.03	3.477	0.0109	1.46	6.77
6.5 <sup>d</sup>	$1 \times 10^{-4}$	O	3.87	1.972	0.0049	Fe	1.87	3.480	0.0118	2.17	5.82
6.5	$1 \times 10^{-5}$	O	4.12	1.972	0.0056	Fe	2.10	3.471	0.0131	2.03	6.81
7.5	$1 \times 10^{-3}$	O	3.68	1.977	0.0044	Fe	1.79	3.482	0.0121	0.45	7.47
						Fe <sup>f</sup>	1.37	3.471	0.0110	2.50	10.8
						Zn <sup>f</sup>	0.31	3.537	0.0110		
7.5	$1 \times 10^{-4}$	O	3.87	1.975	0.0051	Fe	1.87	3.477	0.0132	1.32	8.41
						Fe <sup>f</sup>	1.39	3.445	0.0110	0.76	12.3
						Zn <sup>f</sup>	0.26	3.525	0.0110		
7.5	$1 \times 10^{-5}$	O	4.04	1.981	0.0055	Fe	1.97	3.487	0.0115	0.93	7.89
7.5 <sup>e</sup>	$1 \times 10^{-3}$	O	3.85	1.985	0.0037	Fe	1.23	3.501	0.0110	1.35	3.81
						Zn	1.17	3.546	0.0110		

Note.  $\Gamma$  = sorption density (mol Pb g<sup>-1</sup> ferrihydrite), CN = coordination number,  $R$  = average radial distance,  $\sigma^2$  = Debye–Waller factor:

<sup>a</sup> Uncertainties in coordination numbers are  $\pm 20\%$  for the first shell and  $\pm 20\%$  for the second shell.

<sup>b</sup> Variations in  $R$  are estimated to be 0.03 Å for first shell and 0.05 for second shell.

<sup>c</sup> Errors associated with  $\sigma^2$  are 15% for both shells. All fits obtained using a theoretical model for a Fe-substituted chalcophanite [30].

<sup>d</sup> Sample studied at I.S.  $10^{-3}$  M NaNO<sub>3</sub>.

<sup>e</sup> Coprecipitation sample.

<sup>f</sup> Alternative fits including contributions from Fe and Zn to fit the second shell, where  $\sigma^2$  were constrained equal.

served at lower sorption densities. Then again, at pH  $\geq 6.5$ , Zn(II) ions may begin to form zinc-hydroxide-like polynuclear sorption complexes on the surfaces of ferrihydrite at higher sorption densities. Both macroscopic and spectroscopic studies provide no significant evidence for Zn precipitates over the entire range of reaction conditions employed in this study. Surprisingly, small changes in temperature had a significant impact on the affinity of zinc for the ferrihydrite surface. As temperature fell from 25 to 4 °C for all pH, the equilibrium sorption capacity decreased by 3–4 orders of magnitude. Zinc sorption onto ferrihydrite, therefore is governed by pH as well as by temperature and the sorbate/sorbent ratio. Most importantly, this research asserts that elucidating the reaction mechanisms as well as estimating the associated transport and thermodynamic parameters are crucial for accurately describing the fate of toxic metal pollutants, such as Zn(II), in soils and aquatic ecosystems rich in iron oxides.

## Acknowledgments

Funding from the DuPont Company and the State of Delaware through the Delaware Research Partnership supported this research. The authors gratefully thank the tech-

nical support of staff at X11A, National Synchrotron Light Source, Brookhaven National Laboratory (New York). The authors also thank Dr. Noel Scrivner of DuPont Engineering Technology for his valuable input on this research.

## References

- [1] L. Benyahya, J. Garnier, Environ. Sci. Technol. 33 (1999) 1398.
- [2] R.G. Ford, D.L. Sparks, Environ. Sci. Technol. 34 (2000) 2479.
- [3] D.G. Kinniburgh, M.L. Jackson, J.K. Syers, Soil Sci. Soc. Am. J. 40 (1976) 796.
- [4] M. Okazaki, K. Takamido, I. Yamane, Soil Sci. Plant Nutr. 32 (1986) 523.
- [5] H. Tamura, R. Furuichi, J. Colloid Interface Sci. 195 (1997) 241.
- [6] P. Trivedi, L. Axe, Environ. Sci. Technol. 34 (2000) 2215.
- [7] R.M. McKenzie, Aust. J. Soil Res. 18 (1980) 61.
- [8] M.M. Benjamin, J.O. Leckie, J. Colloid Interface Sci. 79 (1) (1981) 201.
- [9] N.J. Barrow, J. Gerth, G.W. Brümmer, J. Soil Sci. 40 (1989) 437.
- [10] D.P. Rodda, B.B. Johnson, J.D. Wells, J. Colloid Interface Sci. 184 (1996) 365.
- [11] P. Trivedi, L. Axe, J. Colloid Interface Sci. 244 (2001) 221.
- [12] D. Hesterberg, D.E. Sayers, W. Zhou, G.M. Plummer, W.P. Robarge, Environ. Sci. Technol. 31 (1) (1997) 2840.
- [13] S.A. Carroll, P.A. O'Day, M. Piechowski, Environ. Sci. Technol. 32 (1998) 956.
- [14] P.A. O'Day, S.A. Carroll, G.A. Waychunas, Environ. Sci. Technol. 32 (1998) 943.

- [15] M.D. Buatier, S. Sobanska, F. Elsass, *Appl. Geochem.* 16 (2001) 1165.
- [16] D.R. Roberts, A.C. Scheinost, D.L. Sparks, *Environ. Sci. Technol.* 36 (2001) 1742.
- [17] M. Isaure, A. Laboudigue, A. Manceau, G. Sarret, C. Tiffreau, P. Trocellier, G. Lamble, J. Hazemann, D. Christopher, *Geochim. Cosmochim. Acta* 66 (2002) 1549.
- [18] L.M. Shuman, *Soil Sci. Soc. Am. J.* 41 (1977) 703.
- [19] P.R. Anderson, M.M. Benjamin, *Environ. Sci. Technol.* 19 (1985) 1048.
- [20] P. Trivedi, L. Axe, T.A. Tyson, *J. Colloid Interface Sci.* 244 (2001) 230.
- [21] P. Trivedi, L. Axe, T.A. Tyson, *Environ. Sci. Technol.* 35 (2001) 4515.
- [22] T.P. Trainor, G.E. Brown Jr., G.A. Parks, *J. Colloid Interface Sci.* 231 (2000) 359.
- [23] M.L. Schlegel, A. Manceau, L. Charlet, *J. Phys. IV Fr.* 7C-3 (1997) 823.
- [24] G.A. Waychunas, C.C. Fuller, J.A. Davis, *Geochim. Cosmochim. Acta* 66 (2002) 1119.
- [25] E.J. Elzinga, R.J. Reeder, *Geochim. Cosmochim. Acta* 66 (2002) 3943.
- [26] G. Brümmer, J. Gerth, K.G. Tiller, *J. Soil Sci.* 39 (1988) 37.
- [27] J.A. Dyer, P. Trivedi, N.C. Scrivner, D.L. Sparks, submitted for publication.
- [28] J.A. Dyer, P. Trivedi, S.J. Sanders, N.C. Scrivner, D.L. Sparks, submitted for publication.
- [29] P. Trivedi, J.A. Dyer, D.L. Sparks, *Environ. Sci. Technol.* 37 (2003) 908.
- [30] A.C. Scheinost, S. Abend, K.I. Pandya, D.L. Sparks, *Environ. Sci. Technol.* 35 (2001) 1090.
- [31] J.D. Allison, D.S. Brown, K.J. Novo-Gradac, MINTEQA2/PRODEFA2: A Geochemical Assessment Model for Environmental System., Center for Exposure Assessment Modeling, U.S. EPA, 1991.
- [32] J.E. Post, D.E. Appleman, *Am. Mineral.* 73 (1988) 1401.
- [33] D.A. Dzombak, F.M.M. Morel, *Surface Complexation Modeling: Hydroxide Ferric Oxide*, Wiley, New York, 1990.
- [34] M. Padmanabhan, *Aust. J. Soil Res.* 21 (1983) 515.
- [35] P.R. Anderson, M.M. Benjamin, *Environ. Sci. Technol.* 24 (1990) 692.
- [36] N.Z. Misak, H.F. Ghonemy, T.N. Morcos, *J. Colloid Interface Sci.* 184 (1996) 31.
- [37] L.J. Criscenty, D.A. Sverjensky, *J. Colloid Interface Sci.* 253 (2002) 329.
- [38] H.S. Fogler, *Elements of Chemical Engineering*, 2nd ed., Prentice-Hall, Englewood Cliffs, NJ, 1992.
- [39] S. Lin, R. Juang, *J. Haz. Mater. B* 92 (2002) 315.
- [40] B. Bayat, *Water Air Soil Pollut.* 136 (2002) 69.
- [41] B.B. Johnson, *Environ. Sci. Technol.* 24 (1990) 112.
- [42] M.J. Angove, B.B. Johnson, J.D. Wells, *J. Colloid Interface Sci.* 204 (1998) 93.
- [43] C. Zhu, *Chem. Geol.* 188 (2002) 23.
- [44] G.A. Waychunas, C.C. Fuller, J.A. Davis, J.J. Rehr, *Geochim. Cosmochim. Acta* 67 (2003) 1031.
- [45] D.T. Harvey, R.W. Linton, *Colloids Surf.* 11 (1984) 81.
- [46] A. Manceau, M.L. Schlegel, M. Musso, V.A. Sole, C. Gauthier, P.E. Petit, F. Trolard, *Geochim. Cosmochim. Acta* 64 (2000) 3643.